Polaron master equation theory and design of an on-demand quantum dot single-photon source through cavity-assisted stimulated adiabatic Raman passage

Chris Gustin

Queen's University, Department of Physics, Engineering Physics and Astronomy

Supervisor: Dr. Stephen Hughes

Introduction and Motivation

Single-photon sources are an integral part of numerous proposals in the emerging fields of quantum information processing and nanotechnology, including quantum computing and quantum cryptography. These schemes typically require quantum light sources which can emit indistinguishable single-photons on-demand with high efficiency.

One promising candidate for single-photon sources is a quantum dot (QD) inside a photonic cavity. QDs are nanoscale semiconductor objects in which excited electron-hole pairs (excitons) mimic the excited states of an atom. QDs can be exploited to emit photons into a cavity after pulse triggering, allowing for them to be used as single-photon sources. However, the solid-state nature of the QD means that phonons (most importantly longitudinal acoustic (LA) phonons) intrinsically couple to the exciton states, adding a rich and complex interaction to the source excitation dynamics. Notably, phonons cause decoherence, typically degrading the figures-of-merit for practical single-photon sources.

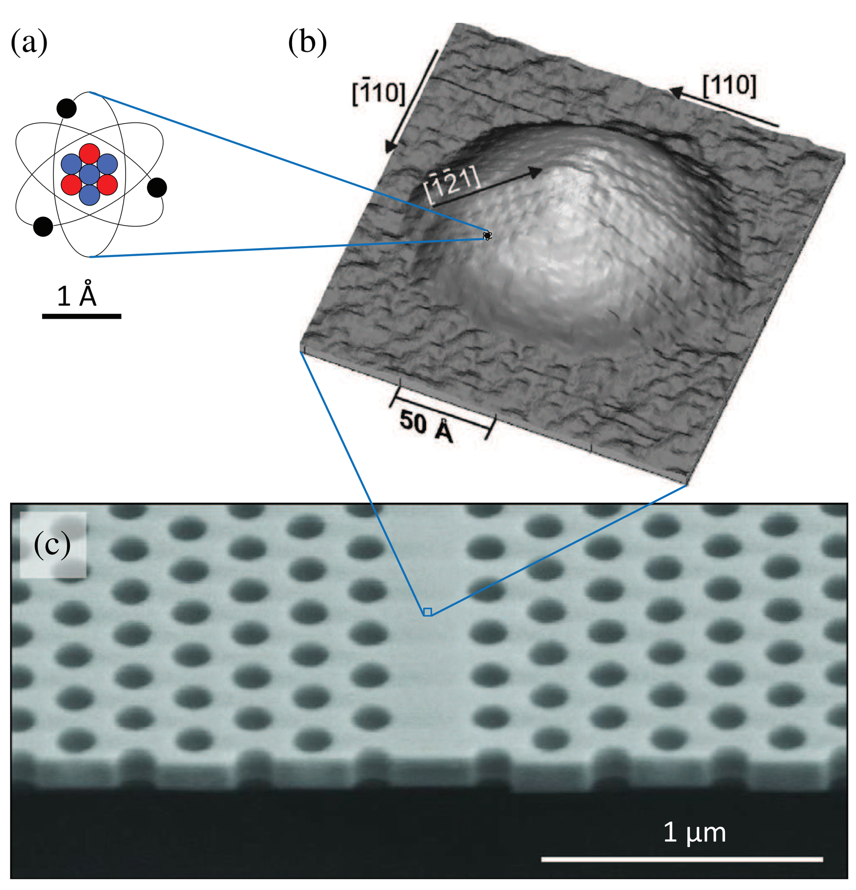

Fig. 1: Schematic of a QD embedded in a photonic crystal waveguide, including typical characteristic length scales. (a) The atomic composition of a QD. (b) A scanning tunneling microscopy image of a self-assembled InGaAs QD. (c) A scanning electron microscopy image of a photonic crystal waveguide, with the location a QD could be embedded highlighted. Figure ((a) and (c)) from Ref. [1]; (b) from Ref. [2].

In this work, we extend a theoretical proposal by Pathak and Hughes (Ref. [3]) which uses stimulated adiabatic Raman passage (STIRAP) and the QD biexciton-exciton cascade as a QD-cavity single-photon source, by adding into the analysis a rigorous model of LA phonon interactions.

Project Goals

- Investigate effects of LA phonon-exciton coupling on efficiency and indistinguishability of emitted photons
- Perform parameter sweep of laser and cavity detunings to optimize efficiency of source in presence of phonons
- Explore effects of temperature variation
- Develop efficient computational model to solve master equation

Biexciton Cascade and STIRAP

We model the QD energy levels as a four-level system (biexciton-exciton cascade) consisting of ground state $|g\rangle$, X and Y linearly polarized excitons $|X\rangle$ and $|Y\rangle$, and biexciton (two excitons) state $|XX\rangle$ with energy levels $\hbar\omega_g = 0$, $\hbar\omega_X$, $\hbar\omega_Y$, and $\hbar\omega_{XX}$, respectively. We treat a cavity mode at the system level with creation (destruction) operators $\hat{a}^\dagger$ ($\hat{a}$).

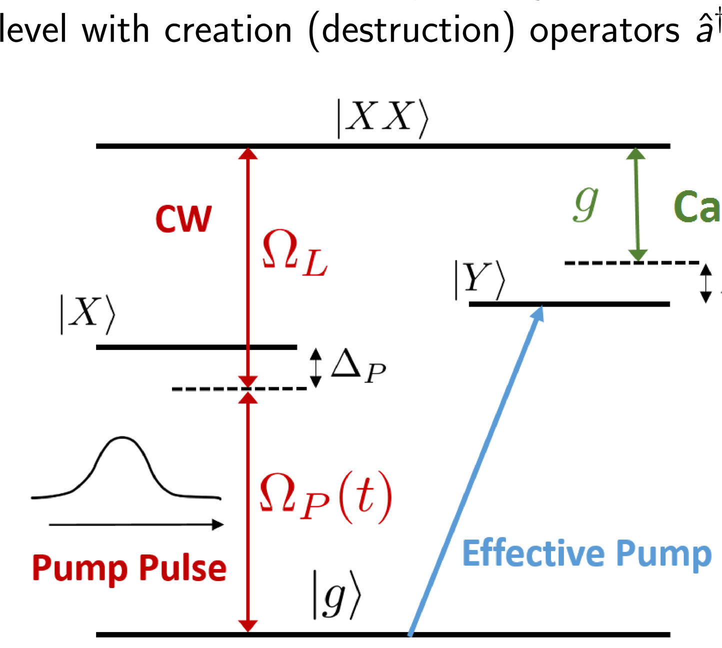

Fig. 2: STIRAP scheme within the biexciton cascade. A pump pulse couples the ground-to-X-exciton transition with detuning Δ_P. A CW laser couples the exciton-biexciton state with detuning $\Delta_P + \Delta_L = 0$ to satisfy the two-photon resonance condition. A cavity couples the biexciton state to the Y-exciton with detuning Δ_C. By design, the biexciton and X-exciton states are never significantly populated owing to the STIRAP process.

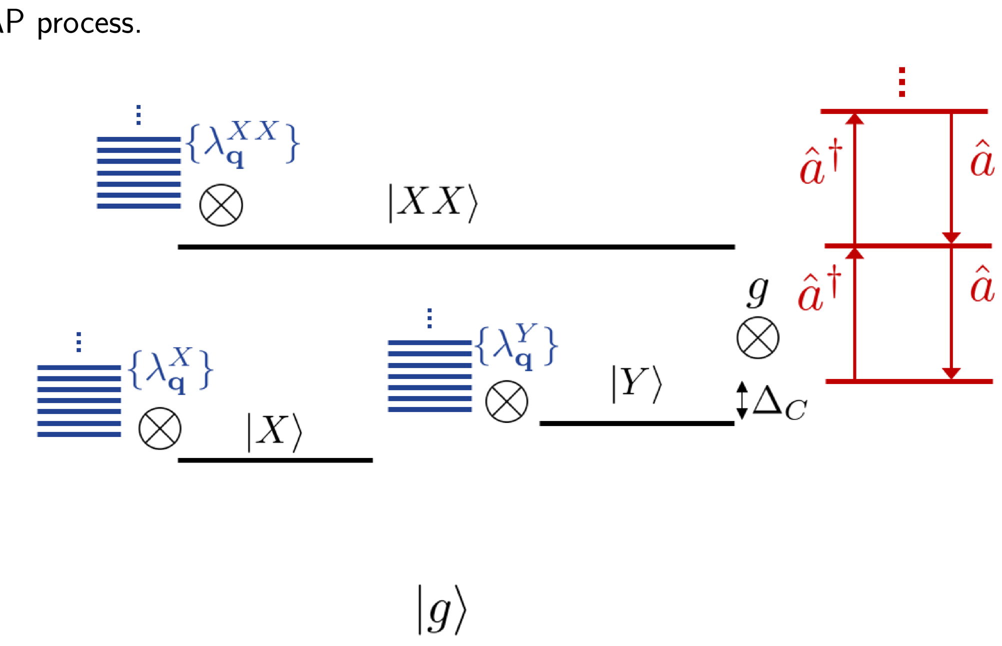

Fig. 3: State space studied in this work – biexciton cascade with phonon and cavity coupling. Each excited state is coupled to a bath of phonon (bosonic) modes with a set of coupling constants (assumed real) $\{\lambda_{\mathbf{q}}^X\}$, $\{\lambda_{\mathbf{q}}^Y\}$, and $\{\lambda_{\mathbf{q}}^{XX}\}$.

Modelling

Polaron transform is applied to treat phonon-exciton coupling nonperturbatively over a wide range of temperatures [4].

Polaron system Hamiltonian:

$$\hat{H}'_S = \hbar\Delta_P |X\rangle\langle X| - \hbar\Delta_C |Y\rangle\langle Y| - \hbar\langle B\rangle\Big[\Omega_L |XX\rangle\langle X| + \Omega_P(t)|X\rangle\langle g| + g|XX\rangle\langle Y|\hat{a} + \text{H.c.}\Big], \quad (1)$$

with CW laser $\Omega_L = 250$ GHz and cavity-exciton coupling $g = 50$ GHz. Pump pulse, CW drive and cavity coupling are coherently modified by the phonon bath displacement $\langle B\rangle$:

$$\langle B\rangle = \exp\left[-\frac{1}{2}\int_0^\infty \frac{J(\omega)}{\omega^2}\coth\left(\frac{\beta\hbar\omega}{2}\right)\right]. \quad (2)$$

Phonon spectral distribution $J(\omega) = \alpha\omega^3 e^{-\frac{\omega^2}{2\omega_b^2}}$ quantifies strength of InGaAs/GaAs QD LA phonon-exciton coupling with $\alpha = 0.03$ ps^2 and $\hbar\omega_b = 0.9$ meV, similar to experimental results in Ref. [5]. Unless stated otherwise, $T = 5$ K.

The system evolution is modelled using an open quantum system master equation approach in the density matrix formalism. We derive a time-local master equation using a 2nd-order Born-Markov approximation:

$$\frac{d}{dt}\rho(t) = -\frac{i}{\hbar}[\hat{H}'_S,\rho(t)] - \frac{1}{\hbar^2}\int_0^\infty d\tau \sum_{m=\{g,u\}} \left(G_m(\tau)[\hat{X}_m(t),\hat{X}_m(t,\tau)\rho(t)] + \text{H.c.}\right) + \sum_\mu \mathcal{L}[\hat{O}_\mu]\rho(t), \quad (3)$$

with drive operators

$$\hat{X}_g = \hbar\Omega_P(t)|X\rangle\langle g| + \hbar\Omega_L|XX\rangle\langle X| + \hbar g|XX\rangle\langle Y|\hat{a} + \text{H.c.} \quad (4)$$

$$\hat{X}_u = i\Big(\hbar\Omega_P(t)|X\rangle\langle g| + \hbar\Omega_L|XX\rangle\langle X| + \hbar g|XX\rangle\langle Y|\hat{a}\Big) + \text{H.c.}, \quad (5)$$

$\hat{X}_m(t,\tau) \equiv e^{-i\hat{H}'_S\tau/\hbar}\hat{X}_m(t)e^{i\hat{H}'_S\tau/\hbar}$, and phonon Green functions

$$G_g(\tau) = \langle B\rangle^2[\cosh(\phi(\tau)) - 1] \quad (6)$$

$$G_u(\tau) = \langle B\rangle^2\sinh(\phi(\tau)), \quad (7)$$

where

$$\phi(\tau) = \int_0^\infty d\omega\frac{J(\omega)}{\omega^2}\left(\coth\left(\frac{\beta\hbar\omega}{2}\right)\cos(\omega\tau) - i\sin(\omega\tau)\right). \quad (8)$$

Other decohering phenomena incorporated through Lindblad collapse operators $(\hat{O})$ of the form $\mathcal{L}[\hat{O}]\rho(t) = \hat{O}\rho\hat{O}^\dagger - \frac{1}{2}\{\hat{O}^\dagger\hat{O},\rho\}$, with $\sqrt{\gamma_1}|X\rangle\langle XX|$, $\sqrt{\gamma_1}|Y\rangle\langle XX|$, $\sqrt{\gamma_2}|g\rangle\langle X|$, and $\sqrt{\gamma_2}|g\rangle\langle Y|$ for spontaneous emission; $\sqrt{2\gamma_d}|XX\rangle\langle XX|$, $\sqrt{\gamma_d}|X\rangle\langle X|$, and $\sqrt{\gamma_d}|Y\rangle\langle Y|$ for pure dephasing; and $\sqrt{\kappa}\hat{a}$ for cavity leakage, with $\gamma_1 = \gamma_2 = 0.5$ GHz, $\kappa = 25$ GHz, and $\gamma_d = 1$ GHz except where stated otherwise. The efficiency is quantified by the emitted cavity photon number, $N_e \equiv \lim_{t\to\infty}\int_0^t d\tau\kappa\langle\hat{a}^\dagger\hat{a}\rangle(\tau)$.

Quantum indistinguishability ($\mathcal{I}$) is quantified by simulating a Hong-Ou-Mandel interferometry set-up [6]:

$$\mathcal{I} \equiv \lim_{T\to\infty}\frac{1}{2}\left[1 + \frac{\int_0^T dt\int_0^{T-t} d\tau\left[g^{(2)}(t,\tau) - |g^{(1)}(t,\tau)|^2\right]}{\int_0^T dt\int_0^{T-t} d\tau\langle\hat{a}^\dagger\hat{a}\rangle(t)\langle\hat{a}^\dagger\hat{a}\rangle(t+\tau)}\right], \quad (9)$$

with quantum two-time correlation functions $g^{(1)}(t,\tau) = \langle\hat{a}^\dagger(t)\hat{a}(t+\tau)\rangle$ and $g^{(2)}(t,\tau) = \langle\hat{a}^\dagger(t)\hat{a}^\dagger(t+\tau)\hat{a}(t+\tau)\hat{a}(t)\rangle$.

Computational Methods

- Quantum Optics Toolbox for MATLAB [7]
- Master equation solved numericallly with external ODE (RK4) solver
- Two-time correlation functions found with master equation solver by use of the quantum regression theorem

Results

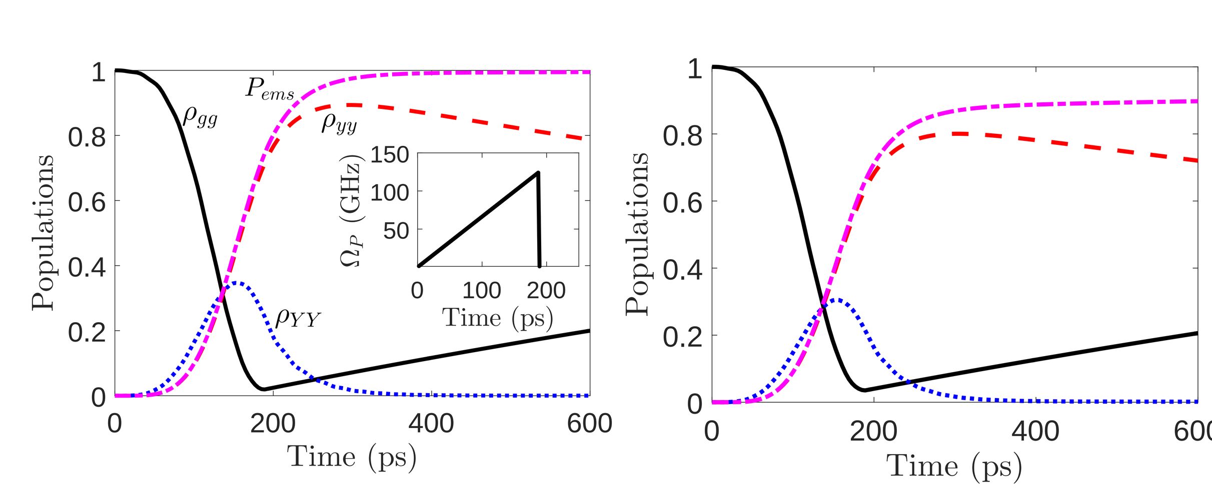

Fig. 4: Populations of states $|g\rangle\otimes|0\rangle$ (ρ_{gg}; black line), $|Y\rangle\otimes|0\rangle$ (ρ_{yy}; red dashed), and $|Y\rangle\otimes|1\rangle$ (ρ_{yy}; blue dotted), where $|0\rangle$ ($|1\rangle$) denotes the cavity number state with 0 (1) photons for the QD-cavity system. Also plotted is the expected number of photons emitted from the cavity (P_{ems}; magenta chain). The pure dephasing rate (of the zero phonon line) is $\gamma_d = 0.5$ GHz. The pump pulse (used throughout) is a single period of a sawtooth wave with maximum amplitude $\Omega_{max} = 2.5g$ and pulse width $g\tau_P = 3\pi$, where $g = 50$ GHz (inset). (a) Populations without phonons, in agreement with Ref. [3]. (b) Populations with acoustic phonon coupling at $T = 5$ K.

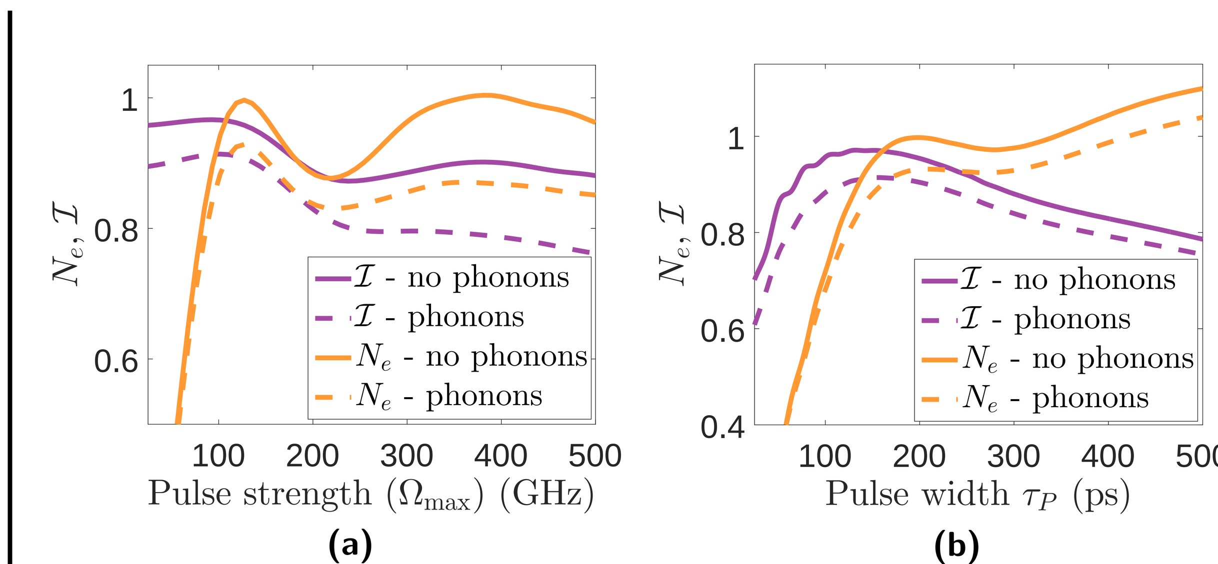

Fig. 5: Indistinguishability and emitted photons for resonant excitation ($\Delta_P = \Delta_C = 0$) vs. (a) max pulse strength and (b) pulse width, with and without phonons.

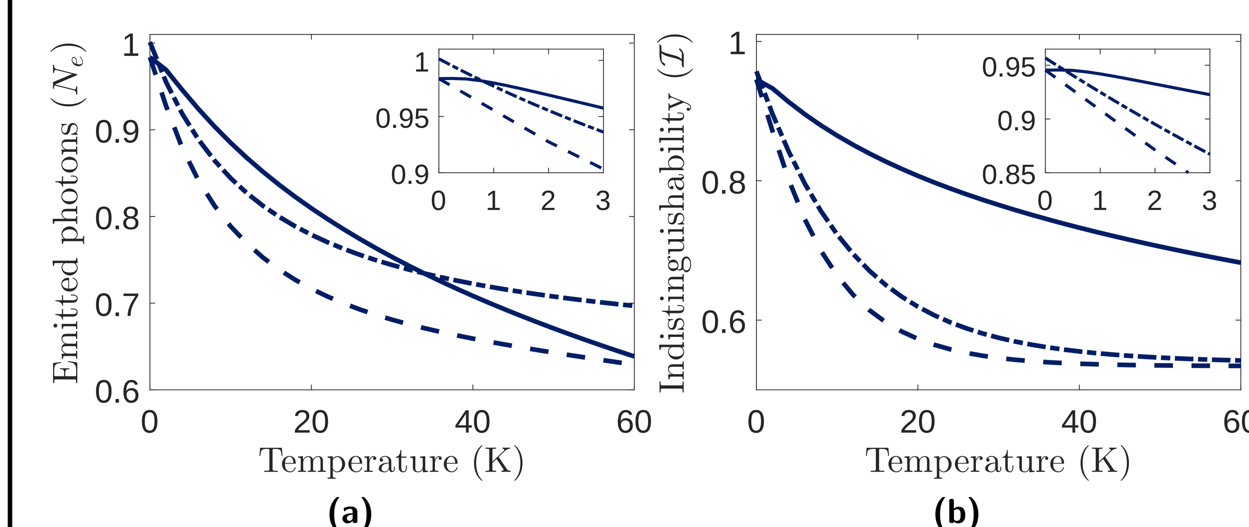

Fig. 6: (a) Emitted photons and (b) indistinguishability as a function of temperature with phonons and constant dephasing $\gamma_0 = 1$ GHz (solid line), with a temperature-dependent dephasing $\gamma_d(T) = 1$ GHz + (2.127 GHz/K)T (following experimental results in Ref. [8]) and no phonons (dash-dotted line), and with both phonons and a temperature-variable dephasing (dashed line). $\Delta_P = \Delta_C = 0$.

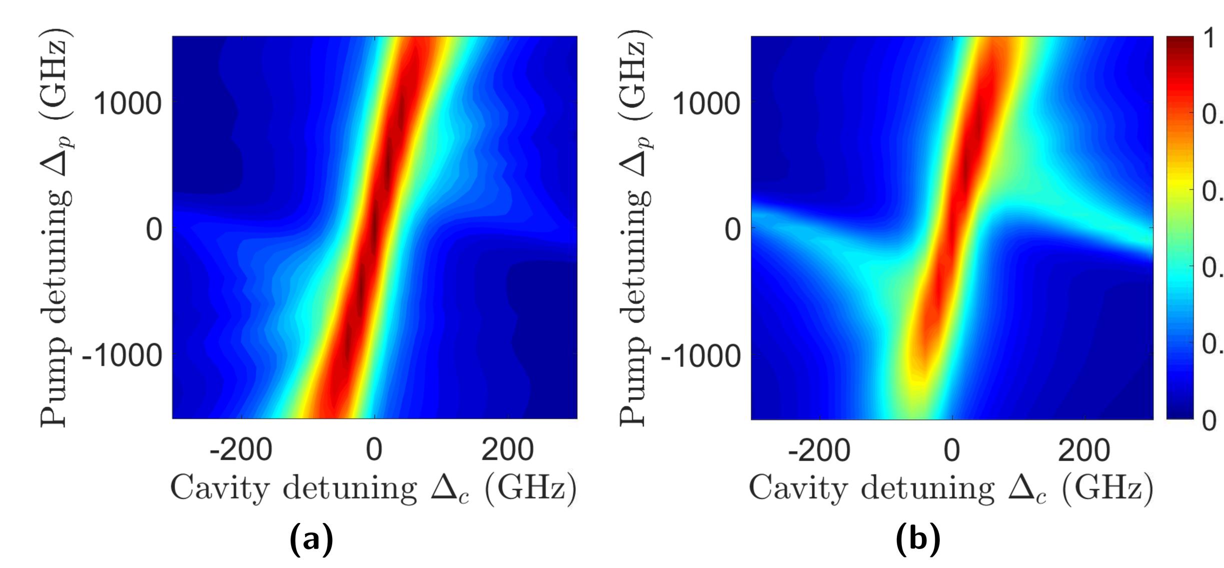

Fig. 7: Emitted cavity photon number N_e plotted as a function of pump pulse detuning Δ_P and cavity detuning Δ_C, with (a) no phonons and (b) phonons. Phonon-mediated off-resonant excitation is clearly seen, and is expected to increase with pump strength [9].

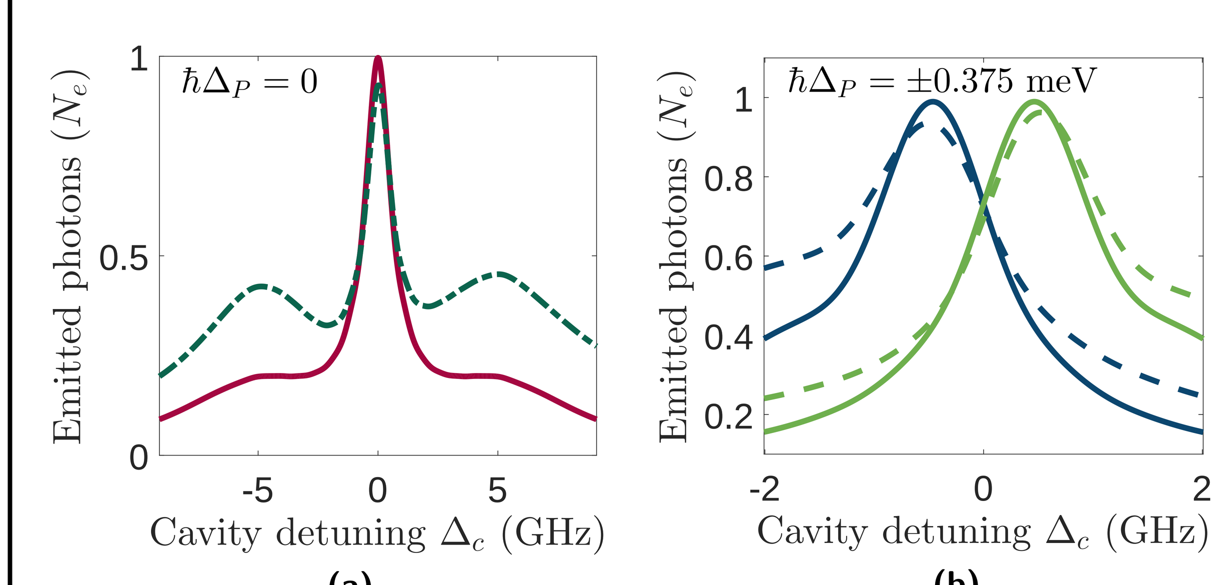

Fig. 8: Emitted photon number as function of cavity detuning for (a) resonant pulse without phonons (red solid line) and with (green dash-dotted line), and (b) off-resonant pump pulse detuned by $\hbar\Delta_P = 0.375$ meV (green), and $\hbar\Delta_P = -0.375$ meV (blue), without phonons (solid line) and with (dashed line).

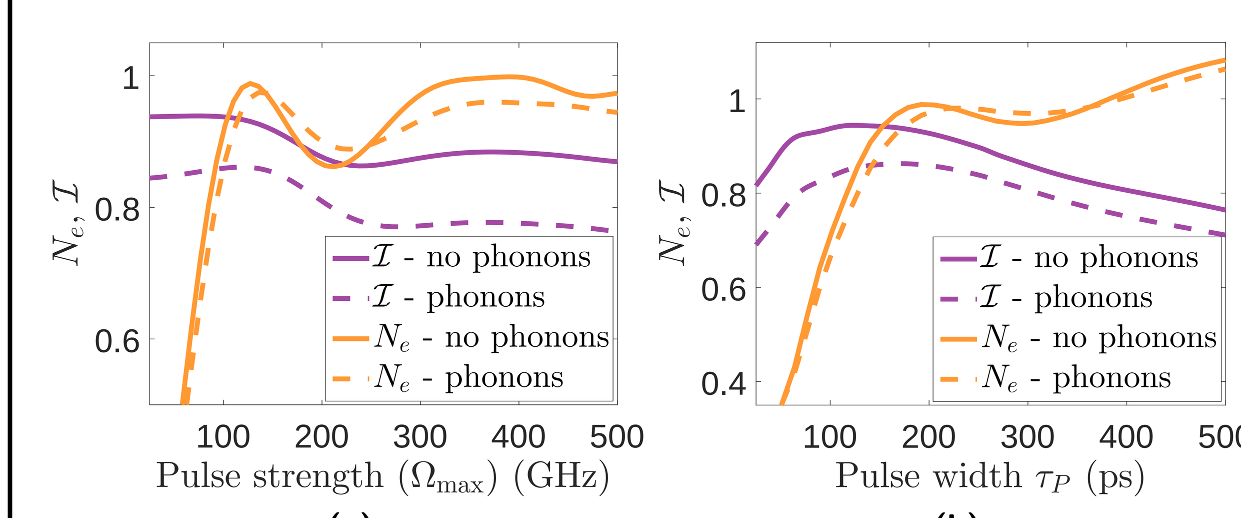

Fig. 9: Indistinguishability and emitted cavity photon number for off-resonant excitation ($\hbar\Delta_P = 0.375$ meV; $\hbar\Delta_C = 0.0165$ meV) optimized for max N_e as a function of (a) max pulse strength and (b) pulse width, with and without phonons.

Conclusions

- Over 90% efficiency and indistinguishability simultaneously achievable on-resonance for realistic experimental parameters
- Most effects of temperature (even at ~ 4 K) are due to pure dephasing (reducible experimentally), not fundamental phonon limits
- Off-resonant excitation allows for near unity (98%) efficiency, but at the cost of only $\sim 86\%$ indistinguishability (Fig. 9)

References

[1] P. Lodahl, S. Mahmoodian, and S. Stobbe, Rev. Mod. Phys. **89**, 347 (2015).
[2] J. Márquez, L. Geelhaar, and K. Jacobi, Appl. Phys. Lett. **78**, 2309 (2001).
[3] P. K. Pathak, and S. Hughes, Phys. Rev. B **82**, 045308 (2010).
[4] D. P. S. McCutcheon and A. Nazir, New J. Phys. **12**, 113042 (2010).
[5] J. H. Quilter *et.al.*, Phys. Rev. Lett. **114**, 137401 (2015).
[6] A. Kiraz, M. Atatüre, and A. Imamoglū, Phys. Rev. A **69**, 032305 (2004).
[7] S. M. Tan, A Quantum Optics Toolbox for Matlab 5, 2002: http://qo.phy.auckland.ac.nz/toolbox/
[8] Y. Ota, S. Iwamoto, N. Kumagai, and Y. Arakawa, 2009 (unpublished). arXiv: 0908.0788
[9] R. Manson, K. Roy-Choudhury, and S. Hughes, Phys. Rev. B **93**, 155423 (2016).

Acknowledgements

I would like to thank my dedicated supervisor, Dr. Stephen Hughes, and always helpful fellow research group members, in particular Dr. Nishan Mann and Ross Manson for their technical assistance.